Probing dynamics of nanoparticle chains formation during magnetic hyperthermia using time-dependent high-frequency hysteresis loops

N Mille, D de Masi, S Faure, J. M. Asensio, B Chaudret, J Carrey

Probing dynamics of nanoparticle chains formation during magnetic hyperthermia using time-dependent high-frequency hysteresis loops

N. Mille, D. De Masi, S. Faure, J.M. Asensio[$], B. Chaudret, J. Carrey*

Université de Toulouse; INSA; UPS; LPCNO (Laboratoire de Physique et Chimie des Nano-Objets), 135 avenue de Rangueil, F-31077 Toulouse, France and CNRS; UMR 5215; LPCNO, F-31077 Toulouse, France

[$] Present adress : Catalysis, Biocatalysis and Separation Division, IFP Energies Nouvelles, Rond-point de l'échangeur de Solaize BP 3, 69360 Solaize, France

Abstract:

The heating power of magnetic nanoparticles (MNPs) submitted to high-frequency magnetic fields is generally probed using calorimetric methods, which supposes that heating power does not evolve with time. Among the several parameters governing MNP heating properties, their organization into chains under the influence of the applied magnetic field is of key importance, though the dynamic of this phenomenon has been rarely studied experimentally. In the present article, time-resolved high-frequency hysteresis loops are used to probe the dynamics of chain formation on a sample of 17.3±2.2 nm $FeNi_3$ MNPs. Chains are formed on a time scale which strongly depends on magnetic field amplitude, ranging from several tens of seconds to less than 100 ms, but do not depend on frequency in the range studied here (from 9 to 78 kHz). Both heating power and hysteresis loop squareness increase with time as chains progressively form. These findings have important methodological consequences when defining protocols or analysing data issued from calorimetric measurements since, in samples where chains form, heating power varies on a time scale which can be comparable to typical measurement times.

Main Text:

Maximizing the specific absorption rate (SAR) of nanoparticles in magnetic hyperthermia and interpreting experimental results is a complex task, since the magnetic properties of assemblies of magnetic nanoparticles (MNPs) depend on a large number of parameters. In particular cases when MNPs can be considered as single-domain, fixed, and magnetically independent, underlying mechanisms are now well-understood [1, 2]. However, the presence of magnetic interactions and the possibility for the MNPs to rotate physically or to self-organize when they are dispersed in a fluid increase the complexity of the problem. One major point, which has led to many theoretical and experimental studies, is the fact that MNPs, under the influence of the field used in magnetic hyperthermia, tend to form chains or columns along the magnetic field direction, which has been proved to enhance the MNP heating power [3, 4, 5, 6, 7, 8, 9, 10, 11, 12, 13, 14].

Chantrell *et al*. pioneered the theoretical approach of the problem in 1982 by calculating the structural properties of chains composed of MNPs of various sizes and showed the

detrimental influence of thermal energy on chain formation [3]. More recently, several studies have been carried out by groups working on magnetic hyperthermia. In particular, the fact that MNP chains display more square hysteresis loops and thus enhanced heating powers has been shown using Monte-Carlo simulations [5, 6], LLG equation [7, 8] or Brownian dynamics simulations [10].

On the experimental side, there is also a general agreement that chains increase the heating power. To demonstrate it, different approaches have been used: in some cases, chains have been formed previously upon using a static magnetic field before being gelled [5, 12, 13], or have been induced by superimposing a static magnetic field to the alternating one during heating power measurements [9]. More specific studies have shown that increasing the thickness of the molecular layer of ligands surrounding the particles limits chain formation [6], as well as the use of a low-viscosity medium [5]. Finally, analysis of high-frequency hysteresis loops measurements seems to indicate that chains are formed only above a critical field, as detected by an increase of magnetic susceptibility [11].

The dynamics of chain formation is an emerging research topic on which a limited number of experimental works have been published. Chaung *et al*. have measured chain formation dynamics under a static magnetic field based on optical transmittance measurements on a ferrofluid [15]. They observed transmittance changes on time scales of several tens of seconds, which was magnetic field amplitude-dependent. However, the optical transmittance alone cannot be easily linked to structural or even more magnetic properties. Recently, Arciniegas *et al.* performed TEM observations of MNPs assembling under very specific conditions. The experiments were performed at zero magnetic field, in the environment of a liquid cell TEM holder, under electron irradiation [16]. So far, the dynamics of chain formation under the typical experimental conditions of magnetic hyperthermia remains largely unexplored.

In the present article, time-resolved high-frequency hysteresis loops are used to probe the dynamics of chain formation. Measurements are based on the fact that formation of chains has clear and visible consequences on the MNP hysteresis loops. Our group published a preliminary result using this methodology, in which a measurement was performed on two samples at a single magnetic field, in order to illustrate that the formation of chains was crucial to understand why two apparently similar samples displayed very different heating properties [14]. In the present article, this technic is pushed forward: magnetic field and frequency-dependant measurements, temperature measurements as well as quantitative analysis are provided. These experiments permit to decorrelate the effects due to chain formation from the ones due to temperature, providing a deeper insight into the physics of this effect.

The MNPs used for this study are $FeNi_x$ NPs, which have been initially developed as heating agents for magnetically induced catalysis; their synthesis is detailed elsewhere [17]. The sample measured in the present study has been synthesized in mesitylene at 150°C during 24 h, with an organometallic precursor ratio Fe/Ni of 1/5, using hexadecylamine and palmitic acid as ligands. The obtained MNP are not perfectly spherical and display an average diameter of 17.3 ± 2.2 nm [see Fig. 1(a)]. Their structural and magnetic properties have been obtained through energy-dispersive X-Ray spectroscopy in a high-resolution transmission electron microscope (HRTEM-EDX), electron energy loss spectroscopy (EELS) analysis, powder X-Ray Diffraction (XRD) as well as vibrating sample magnetometer (VSM). The MNPs possess an fcc structure, and they are composed of a $FeNi_3$ core surrounded by an extremely thin layer of Fe and display a saturation magnetization at 300 K of 80 Am^2kg^{-1}. They are magnetically soft, with a coercive field at 5 K of ca. 5 mT.

In the sample measured here, the MNPs were dispersed in mesitylene at a concentration of 20.6 g/L. When submitted to a high-frequency magnetic field, these MNPs in this sample tend to efficiently organize to form chains, which in some cases are visible with the naked eye [see Fig. 1(b)]. Moreover, the process is easily reversible and after several minutes in an ultrasound bath the chains are completely redissolved, and one recovers a colloidal solution composed of well dispersed MNPs. Thus, we consider that this sample is a good model to deeply study the chain formation phenomenon.

The setup used to generate the alternating magnetic field and to measure the high-frequency hysteresis loops has been described in detail in Ref. [18]. It is based on a Litz wire coil generating the field and a system of two pick-up coils to measure sample magnetization and external field. For the measurements, 0.5 mL of the sample were placed in a glass tube, the latter being inserted into the sample holder. The temperature was measured using an optical probe taped on the sample holder.

As described in Ref. [18], the signal from the pick-up coils of our setup was so far measured using an oscilloscope connected to a computer by an usb cable. This did not permit to record the evolution of the hysteresis loops with time. To do so, we replaced this oscilloscope by a numerical oscilloscope card NI-5114 inserted in a PXIe-1073 chassis (National Instrument). This equipment permits to acquire a hysteresis loop every 1 ms which is fast enough in comparison to the dynamics of the studied system. Thus, " $t = 0$ s" refers to the time at which the power amplifier is switched on. However, the magnetic field reaches its nominal value after approximately 2 ms, corresponding to the rise time of the RLC circuit. This means that the curves rated below as « $t = 5$ ms » corresponds to approximately 3 ms after the magnetic field has reached its nominal value. As described in Ref. [18], the two pick-up coils are not perfectly anti-symmetric so a non-null magnetic signal is detected by our setup even in the absence of magnetic sample. This "blank signal" is stable in time. We measured it during the full time of an experiment before each time-dependent measurement. It was then subtracted to the signal measured with the sample in place at the same corresponding time.

Fig. 2(a)-(d) shows the time-evolution of the hysteresis loops measured at 50 kHz for various applied magnetic fields (full dataset can be found in Supplementary Information, Fig.SI-1). Several features can be observed in these data. First, at a magnetic field of amplitude $\mu_0 H_{max} = 9.4$ mT, the hysteresis loops have a very low remnant magnetization, are far from being saturated (minor cycles) and do not evolve with time. Their elliptic shape is typical of superparamagnetic MNPs measured under a low magnetic field responding linearly to the magnetic field excitation [1]. For a field of 18.8 mT, the behavior is very different: just after the magnetic field has been switched on, the hysteresis loop is similar to the one described previously; however, it evolves after a few seconds toward a square shape and fully saturated hysteresis loop typical of ferromagnetic MNPs with their easy axis aligned with the field. We interpret this transition as a consequence of chains formation. Alternative hypotheses will be discussed below. For larger magnetic fields, the behaviour is similar, except that the time to reach this fully saturated state diminishes strongly. For instance, for a field of 54 mT, it is reached in less than 100 ms.

Another feature is also visible in these hysteresis loops: after the fully saturated state has been reached, the coercive field slowly decreases with time. For instance, for a field of 32 mT, the coercive field $\mu_0 H_c$ evolves from 19 mT to 15.5 mT between 4 s and 120 s. This phenomenon will be discussed later, as its origin will be enlightened by additional experiments.

In the square-shaped hysteresis loops measured at high field, oscillations of the magnetization are visible after the magnetization has switched, as emphasized by a black circle in

Fig 2(d). Oscillations are perfectly reproducible, with a frequency of 5.2 MHz and are due to the self-resonance of the pick-up coils, excited by the abrupt change of magnetization. The oscillations are stronger following an abrupt change of voltage in the pick-up coils, and thus for square hysteresis loops and for a large applied field and frequency (which both increase the magnetization rate of change). They are strong in Fig. 2(d) but can be also visible with a smaller amplitude in other figures. Their presence has no influence on our results and on the quantitative analysis which will be presented below.

Finally, integrating the hysteresis area permits to deduce the SAR of the particles, using the equation SAR = $A\,f$, where A is the hysteresis area and f the frequency. The results are shown in Fig. SI-2 for the data set obtained at 50 kHz. This figure evidences that SAR evolves with time and thus that the SAR($\mu_0 H_{\max}$) curve strongly depends on the t value chosen to perform this calculation.

The features described qualitatively above are quantitatively analysed and summarized in Fig. 3. To visualize the evolution of chain formation, we plot in Fig. 3(a) the slope of the magnetization M (i.e. the differential susceptibility) at the coercive field $\mu_0 H_C$, defined mathematically as $\chi = \left.\frac{dM}{dH}\right|_{\mu_0 H_C}$, as a function of time. The differential susceptibility increases dramatically as chains form. Once the chains are formed, this differential susceptibility experiences a slight decrease at around 1s for applied fields higher than 17 mT and then increases again to a maximum value at around 10 s. It finally slowly decreases for longer times. To analyse the dynamics of the chain formation, Fig. 3(b) shows the time necessary for the susceptibility to reach an arbitrary large value corresponding to a square hysteresis loop (here $\chi > 200$, depicted as a black line on Fig. 3(a)). It is observed that this time evolves from 3.7 s for $\mu_0 H_{\max}$ = 17 mT to 36 ms for $\mu_0 H_{\max}$ = 55 mT. Fig. 3(c) shows the time evolution of the coercive field, which displays an evolution quite similar to the one of the differential susceptibility: an increase just after the field has been switched on followed by the bump between around 1 s and 10 s and finally a slow decrease for longer time. We still lack information to understand the bump at around 1 s. However, the slow decrease of both coercive field and differential susceptibility after 10 s could have several origins: i) a slow structural evolution of the chains once they have been formed. For instance, the decrease of coercive field could be due to a slow change in their aspect ratio; ii) the increase of sample temperature. The experiments presented just below will permit to discriminate between these two hypotheses.

A second series of experiments was performed in order to study the influence of the magnetic field frequency on the dynamics of chain formation. Eight experiments were performed for frequencies ranging from 9 kHz to 78 kHz, with $\mu_0 H_{\max}$ = 28 mT. Typical curves are shown in Fig. 2(e) and (f). Full dataset can be found in Supplementary Information, Fig SI-3. Two main conclusions can be drawn from these data. First, the dynamics of chain formation does not seem to depend on frequency. An analysis similar to the one shown in Fig. 3(b) – permitting to extract a typical time for the chain formation as a function of frequency –, shows that the formation time varies indifferently between 200 and 400 ms when frequency varies between 9 kHz and 78 kHz, without any tendency (see Fig. SI-3). Second, the decrease of coercive field after the chains are formed does, on the contrary, clearly depend on frequency, as illustrated in Fig. 4(a): for higher frequencies, the coercive field decreases faster.

The previous observation could be an effect of temperature since the sample heating power, at first approximation, scales linearly with frequency. To check this hypothesis, we performed a deeper analysis of our data. In Fig. 4(b), the coercive field, measured after the chains have been formed, has been plotted as a function of the number of loops, i.e. the frequency times

the time. Since the temperature is proportional to the number of cycles – at least in the linear part of the $T(t)$ curve –, this is an indirect way to represent the evolution of a quantity of interest – here the coercive field – as a function of sample temperature. One can see that all the data for various frequencies fall onto a single universal curve, indicating that the evolution of the coercive field in the experiments performed at various frequencies is likely a temperature effect. Another way to check it is to plot the coercive field directly as a function of sample temperature. Fig. 4(c) shows raw temperature measurements for experiments performed at various frequencies. We emphasize that, as previously discussed elsewhere, for samples with large heating powers such as the one measured here, the time evolution of the temperature is a noisy and weakly reproducible parameter due to convection effects and to strong temperature gradients inside the calorimeter [19]. This explains several features of the curves shown in Fig. 4(c), such as bumps and unexpected crossing between some $T(t)$ curves measured at different frequencies. In Fig. 4(d), the evolution of the coercive field is plotted as a function of the measured temperature of the sample. Here again, a universal curve is observed, in spite that it is less clear than in Fig. 4(b): in such experiments, the number of cycles is a more robust way of estimating sample temperature than direct temperature measurements. In any case, the hypothesis that the frequency-dependence of the coercive field observed in Fig. 4(a) is a temperature effect seems robust. This hypothesis is also coherent with the decrease of susceptibility with time observed in Fig. 3(a) since, according to the Stoner-Wohlfarth model, when single-domain MNPs are aligned with the magnetic field, an increase of temperature reduces both the coercive field and the differential susceptibility at the coercive field (see Fig. 3(a) in Ref. [1]).

Finally, we discuss of two alternative hypotheses which could possibly explain – at least partially – the observed features. The first one is that the changes in hysteresis loops would be due to the alignment of the MNP easy axis along the magnetic field: the particles would at the beginning of the experiment be randomly oriented and would then rotate to get aligned, without chain formation. This hypothesis seems unlikely for two reasons: i) if the particles were randomly oriented, the remnant magnetization would be half the saturation one; it is experimentally observed that it is much lower; ii) the typical time for a rotation of a nanoparticle under the influence of a magnetic field is of the order of the microsecond, much shorter than the timescale of the phenomena detected here [20]. The second hypothesis is that the observed features would be due to a strong increase of the local temperature of the MNPs; the latter would, at the beginning of the experiment, display a coercive field much larger than the applied field, explaining the flat hysteresis loops. Then the local increase in temperature would diminish the coercive field, leading to the square hysteresis loops. This hypothesis is appealing but is in contradiction with the fact that hysteresis loop becomes square within a time which does not depend on frequency (see Fig. SI-3). A local temperature increase would probably be proportional to frequency as the SAR increases when augmenting this parameter. As a conclusion, the formation of chains – that can be visible with the naked eye – is the most plausible explanation for the observed results, the change in the hysteresis loop shape originating from a modification in the interaction (dipolar and possibly exchange) between MNPs. These interactions drive the MNPs, which have a superparamagnetic behavior when isolated, toward a ferromagnetic state.

Our results show that, in samples where chains form, the heating power of MNPs can be time-dependent,. This has metrological consequences since, when using any calorimetric method to estimate the heating power, the latter might depend on measurement time. For instance, if the measurement time is shorter than the chain formation time, this leads to underestimate the heating power that would be reached in the stationary regime, i.e. when the magnetic field is applied for a

long time. This is important in the framework of biological applications, where magnetic fields are applied during several tens of minutes, whereas typical heating power measurement times are of the order of tens of seconds. Finally, the sample that we have chosen for this study is able to form large chains visible with the naked eye. It would be interesting to use the setup and protocol that has been presented here to study and compare samples of different nature, and in particular to study the influence of MNP size and anisotropy on the dynamics of chain formation, since these two parameters govern most magnetic properties of MNPs.

Supplementary materials:

See supplementary material for the complete dataset of chain dynamics with field and frequency presented on Fig. 2.

Acknowledgements:

The authors thank ERC Advanced Grant (MONACAT 2015-694159) for financial support. The authors would like to thank Irene Morales Casero for fruitful discussion and improvement of the setup.

Data availability:

The data that support the findings of this study are available from the corresponding author upon reasonable request.

References:

* Electronic mail: julian.carrey@insa-toulouse.fr

[1] J. Carrey, B. Mehdaoui and M. Respaud, J. Appl. Phys. **109**, 033901 (2011)
[2] N. A. Usov, J. Appl. Phys. **107**, 123909 (2010)
[3] R. W. Chantrell, A. Bradbury, J. Popplewell, and S. W. Charles, J. Appl. Phys. 53, 2742 (1982).
[4] B. Mehdaoui, A. Meffre, L.-M. Lacroix, J. Carrey, S. Lachaize, M. Goujeon, M. Respaud, and B. Chaudret, J. Magn. Magn. Mat. **322**, L49 (2010)
[5] D. Serantes, K. Simeonidis, M. Angelakeris, O. Chubykalo-Fesenko, M. Marciello, M. del P. Morales, D. Baldomir, and C. Martinez-Boubeta, J. of Phys. Chem. C **118**, 5927 (2014).
[6] S. L. Saville, B. Qi, J. Baker, R. Stone, R. E. Camley, K. L. Livesey, L. Ye, T. M. Crawford, and O. Thompson Mefford, J. Colloid Interface Sci. **424**, 141 (2014).
[7] B. Mehdaoui, R. P. Tan, A. Meffre, J. Carrey, S. Lachaize, B. Chaudret, and M. Respaud, Phys. Rev. B **87**, 174419 (2013).
[8] N. A. Usov, M. L. Fdez-Gubieda, and J. M. Barandiarán, J. of Appl. Phys. **113**, 023907 (2013).
[9] S. Ranoo, B. B. Lahiri, T. Muthukumaran, and J. Philip, Appl. Phys. Lett. **115**, 043102 (2019).
[10] Z. Zhao and C. Rinaldi, J. Phys. Chem. C **122**, 21018 (2018).

[11] I. Morales, R. Costo, N. Mille, G. B. da Silva, J. Carrey, A. Hernando, and P. de la Presa, Nanomaterials **8**, 970 (2018).
[12] E. Myrovali, N. Maniotis, A. Makridis, A. Terzopoulou, V. Ntomprougkidis, K. Simeonidis, D. Sakellari, O. Kalogirou, T. Samaras, R. Salikhov, M. Spasova, M. Farle, U. Wiedwald, and M. Angelakeris, Sci Rep **6**, 37934 (2016).
[13] B. Sanz, R. Cabreira-Gomes, T. E. Torres, D. P. Valdes, E. Lima Jr, E. De Biasi, R. D. Zysler, M. Ricardo Ibarra, and G. F. Goya, ACS Appl. Nano Mater. **3**, 8719 (2020).
[14] J. M. Asensio, J. Marbaix, N. Mille, L.-M. Lacroix, K. Soulantica, P.-F. Fazzini, J. Carrey, and B. Chaudret, Nanoscale **11**, 5402 (2019).
[15] M. Chung and C. Fu, IEEE Transactions on Magnetics **47**, 3170 (2011).
[16] M. P. Arciniegas, A. Castelli, R. Brescia, D. Serantes, S. Ruta, O. Hovorka, A. Satoh, R. Chantrell, and T. Pellegrino, Small **16**, 1907419 (2020).
[17] D. De Masi, J. M. Asensio, P.-F. Fazzini, L.-M. Lacroix, and B. Chaudret, Angew. Chem.-Int. Edit. **59**, 6187 (2020).
[18] V. Connord, B. Mehdaoui, R. P. Tan, J. Carrey, and M. Respaud, Review of Scientific Instruments **85**, 093904 (2014).
[19] L.-M. Lacroix, R. B. Malaki, J. Carrey, S. Lachaize, M. Respaud, G. F. Goya, and B. Chaudret, Journal of Applied Physics **105**, 023911 (2009).
[20] D. P. Valdés, E. Lima, Jr., R. D. Zysler, and E. De Biasi, Phys. Rev. Applied 14, 014023 (2020)

Figures:

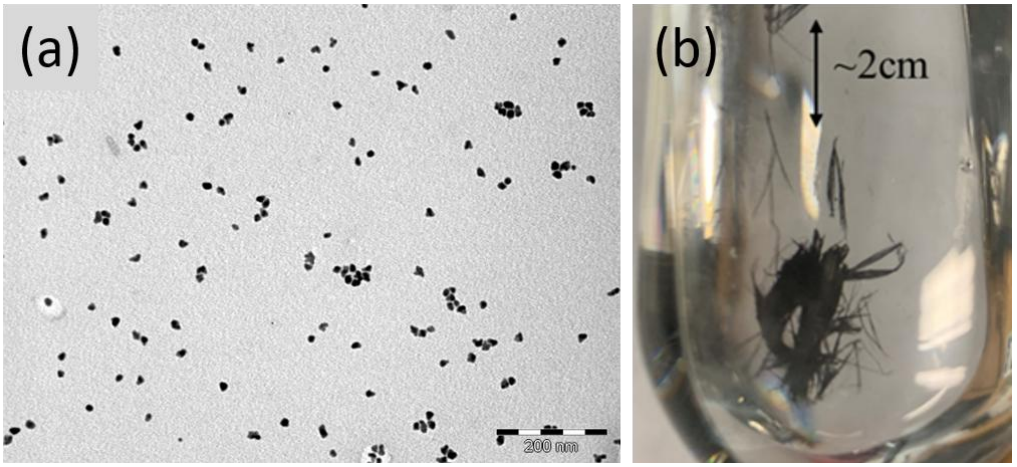

Figure 1: (a) TEM micrographs of the sample. The length of the scale bar is 100 nm. (b) Picture of a similar sample (same synthesis, different batch) after it has been submitted to a 300 kHz and approx. 20 mT field.

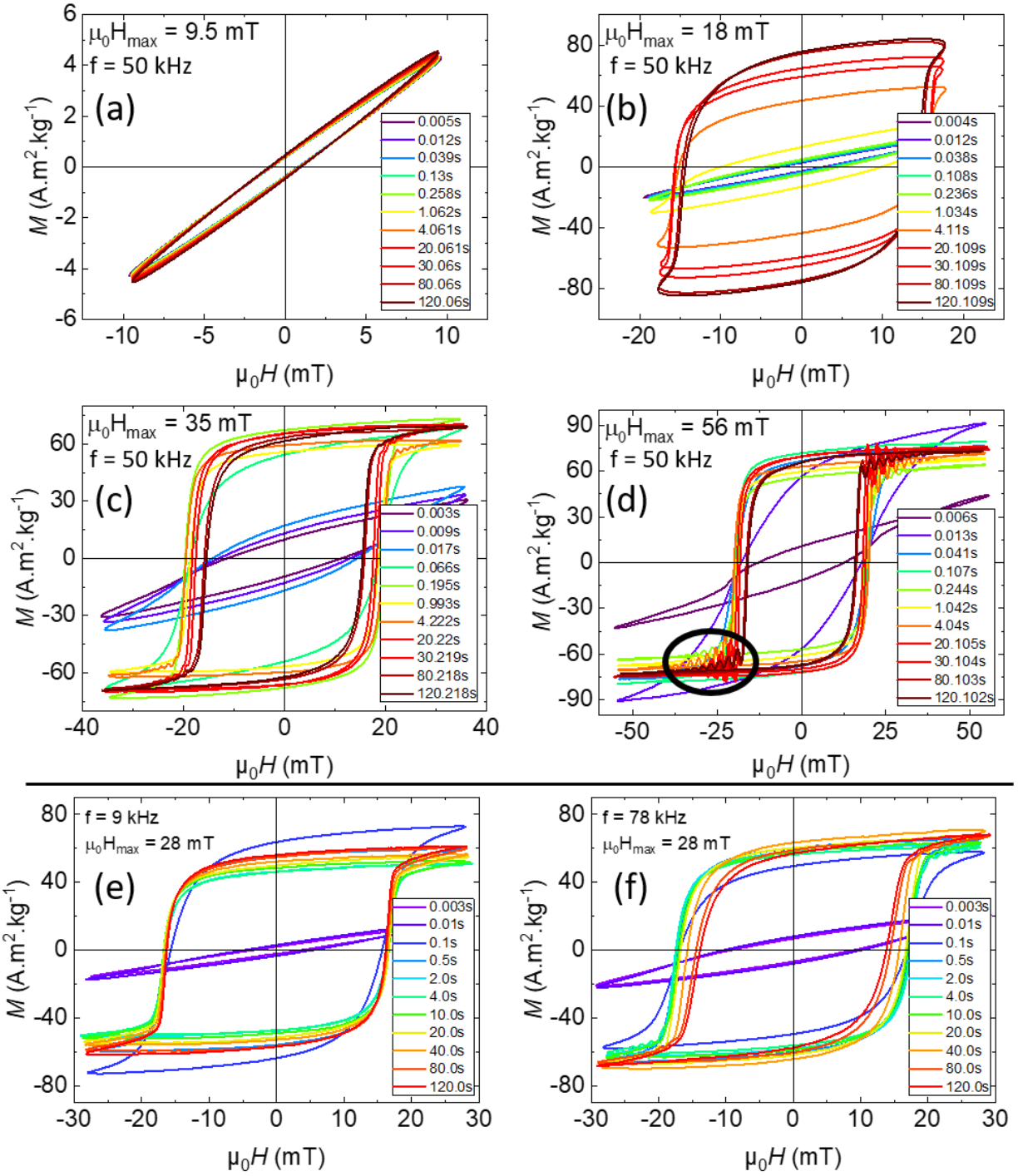

Figure 2: Time evolution of hysteresis loops measured under different applied field condition: (a)-(d) at 50 kHz for different applied magnetic fields, (e) and (f) with $\mu_0 H_{max} = 28$ mT for different frequencies. The times after the field has been switched on as well as the applied magnetic field are specified in the legend. The black circle in (d) emphasizes the self-resonance of the pick-up coils.

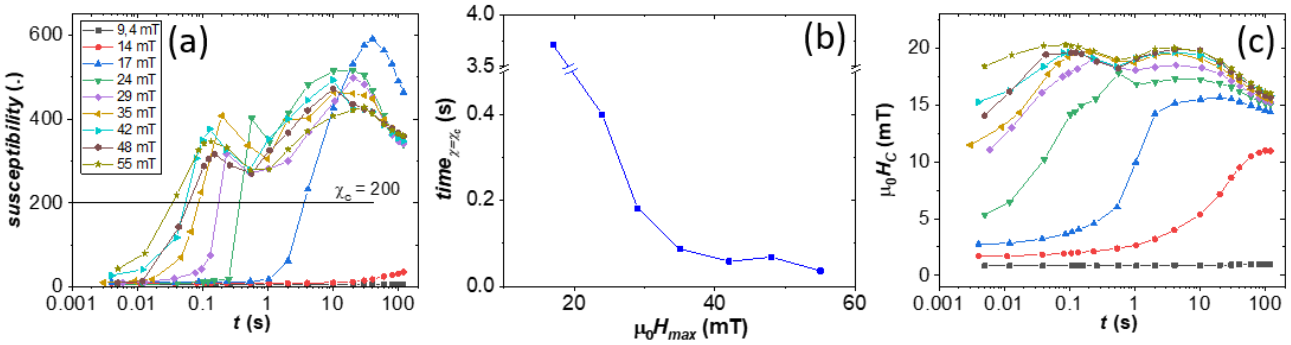

Figure 3 : (a) Time evolution of the hysteresis loop slope (susceptibility) at the coercive field for different applied magnetic fields. (b) Evolution of the time above which the susceptibility at the coercive field exceeds an arbitrary high value (here $\chi > 200$, depicted as a black line on (a)). (c) Time evolution of the coercive field for different applied magnetic fields (share the legend with (a)).

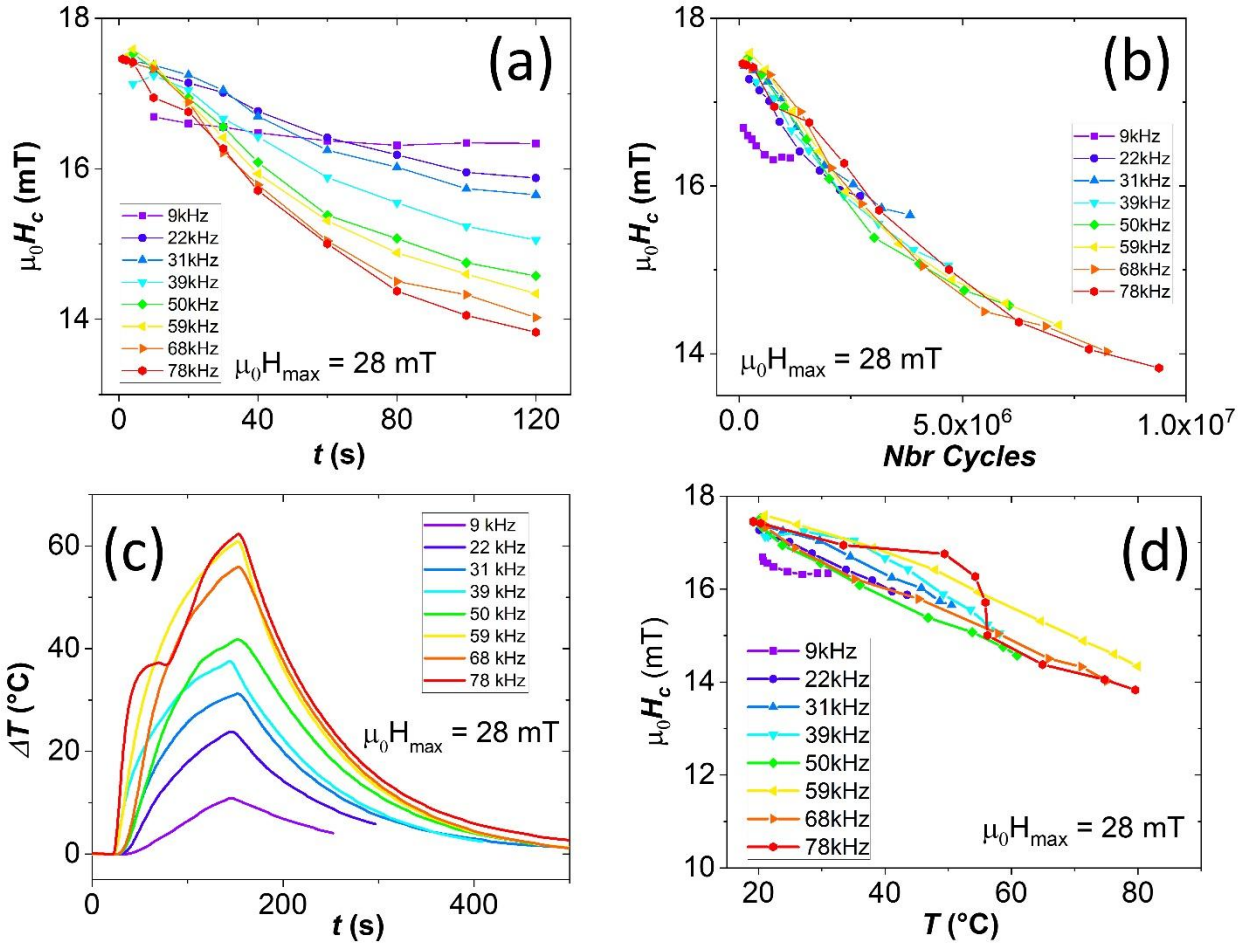

Figure 4 : Evolution of the coercive field for different frequencies as a function of (a) time, (b) number of cycles, (d) temperature. Only coercive field values obtained after the chains have been formed are shown are plotted. (c) Temperature measurements performed in parallel of hysteresis loop measurements.